

Position Control of Rolling Skateboard

Balazs Varszegi* Denes Takacs** Gabor Stepan***

* *Department of Applied Mechanics, Budapest University of Technology and Economics, Budapest, Hungary (e-mail: varszegi@mm.bme.hu)*

** *MTA-BME Research Group on Dynamics of Machines and Vehicles, Budapest, Hungary (e-mail: takacs@mm.bme.hu)*

*** *Department of Applied Mechanics, Budapest University of Technology and Economics, Budapest, Hungary (e-mail: stepan@mm.bme.hu).*

Abstract: A simple mechanical model of the skateboard-skater system is analyzed, in which the skater tries to follow a straight line by the board. The human control is considered by means of a linear delayed PD controller. The equations of motion of the non-holonomic system are derived with the help of the Gibbs-Appell method. The linear stability of the system is given analytically. The effect of the reflex delay of the skater on the stability is investigated. It is shown that in case of zero reflex delay, the motion along a straight line is unstable while non-zero reflex delay can provide stable motion for some specific speed ranges.

Keywords: skateboard, non-holonomic, PD controller, time delay

1. INTRODUCTION

Skateboard has become a popular sport in the 60's. After a decade, the first mechanical model of the skateboard-skater system was constructed by Hubbard (1980). Hubbard's study showed that the mechanical model of the skateboard is a very interesting example of non-holonomic systems. Other researchers also investigated the linear stability of the skateboard-skater system, Kremnev and Kuleshov (2008). All of these studies have provided the same results, the stabilization of the rectilinear motion is easier as the longitudinal speed of the board is increased. Such behavior can commonly be detected in different nonholonomic systems, see, for example, the bicycle or the three-dimensional biped walking machine Wisse and Schwab (2005).

Many practical observations on skateboarding proved, that unwanted loss of stability can also occur at high speed. An explanation for this phenomenon can be originated in the human control, which is always present in the skateboard-skater system. The human control has reflex delay, what can cause unexpected stability losses in case of stick balancing Insperger and Milton (2014) or simple human balancing Stepan (2009). With the extension of Kremnev and Kuleshovs model, it was investigated in Varszegi et al. (2014) how the balancing effort of the skater influences the stability. A linear PD controller was implemented, where the skater's tilting angle was used as the input of the controller. It was verified that the stable parameter domain of the control gains is strongly modified as the longitudinal speed of the board changes, see Figure 1, where the stable parameter domain is rotating around the origin of the $P - D$ plane as the speed increases. Consequently, the skater has to tune the control gains with respect to the speed.

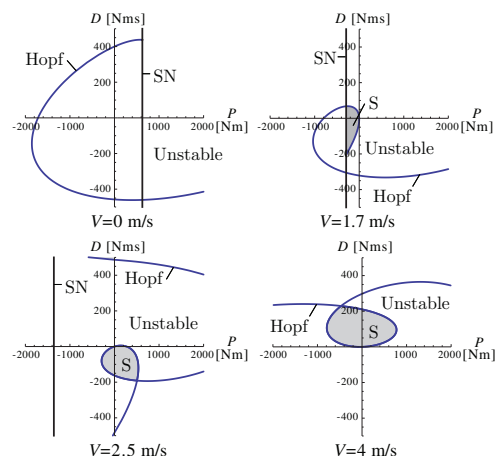


Fig. 1. Linear stability charts for different speeds ¹

In the figure, it can also be observed that the parameter pairs $P = 0$ and $D = 0$ are always at the stability boundary. This means that if the skater switches off its control, the rectilinear motion is just stable. Namely, by means of this simple strategy, the skater could avoid the instability of the board. But this strategy can work if the direction of the rectilinear motion does not matter, namely, the skater does not have to avoid an object on the road and/or does not have to follow the desired path of the road. To investigate the case when the skater has to follow a predefined direction by its board, another control law is needed. In this study, we consider this latter case.

2. NON-HOLONOMIC MECHANICAL MODEL

The mechanical model in question (see Figure 2) is based on Kremnev and Kuleshov (2008) and Varszegi et al.

¹ See in Varszegi et al. (2014)

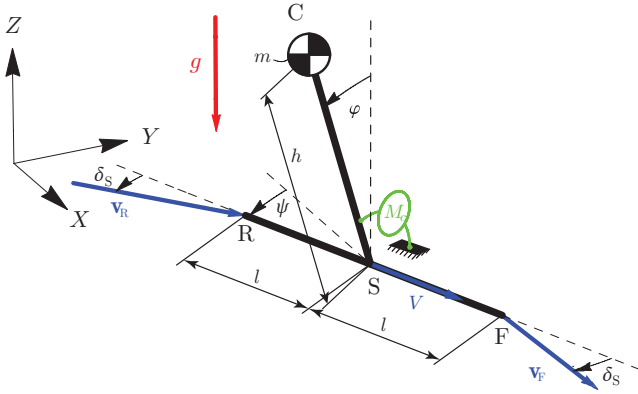


Fig. 2. The simplified mechanical model of the skateboard-skater system

(2014). The skateboard is modeled by a massless rod (between the front axle at F and the rear axle at R) while the skater is represented by a massless rod (between the points S and C) with a lumped mass at C. In this model, the connection between the skater and the board (at S) is assumed to be rigid. The so formed rigid body has zero mass moment of inertia with respect to its center of gravity at C, which makes the derivation of the equations of motion simpler. Namely, the skateboard moves in the three dimensional gravitational field but we have to describe the motion of a lumped mass only.

In our study we do not consider the loss of contacts between the wheels and the ground. Due to the fact that the longitudinal axis of the skateboard is always parallel to the ground, one can choose four generalized coordinates to describe the motion: X and Y are the coordinates of the skateboard center point S in the plane of the ground; ψ describes the direction of the longitudinal axis of the skateboard; and finally, φ is the inclination angle of the skater's body from the vertical direction. The geometrical parameters are the following. The height of the skater is denoted by $2h$. The length of the board is $2l$ while m represents the mass of the skater. The parameter g stands for the gravitational acceleration. Here we model the skater's navigating effort as a linear PD controller, which applies a torque to the skateboard (see Figure 2). The rectilinear motion of the board is prescribed along the $Y = 0$ line, and the control torque is calculated via

$$M_c(t) = -PY(t - \tau) - D\dot{Y}(t - \tau) \quad (1)$$

where τ refers to the time delay, P and D represent the proportional and the differential control gains, respectively. The controller produces zero torque if the board follows the prescribed stationary path.

Regarding to the rolling wheels of the skateboard, kinematic constraints can be formed. These constraining equations define the velocities \mathbf{v}_F and \mathbf{v}_R of the front point (F) and the rear one (R), respectively. The directions of these velocities depend on φ through δ_S , which is the so-called steering angle (see Figure 2). This angle can be expressed from the equation

$$\sin \beta(t) \tan \kappa = \tan \delta_S(t), \quad (2)$$

where κ is the complementary angle of the so-called rake angle in the skateboard wheel suspension (for the derivation of this relation please see Kremnev and Kuleshov

(2008) or Varszegi et al. (2014)). Here we also prescribe the longitudinal speed of the board, which is kept on the constant value V . The so-formed kinematic constraints can be written as

$$\mathbf{A} \cdot \dot{\mathbf{q}} = \mathbf{A}_0, \quad (3)$$

where

$$\mathbf{q}^T = [X \ Y \ \psi \ \varphi], \quad (4)$$

$$\mathbf{A} = \begin{bmatrix} \sin \psi - \cos \psi \sin \varphi \tan \kappa & -\cos \psi - \sin \psi \sin \varphi \tan \kappa & -l & 0 \\ \sin \psi + \cos \psi \sin \varphi \tan \kappa & -\cos \psi + \sin \psi \sin \varphi \tan \kappa & l & 0 \\ \cos \psi & \sin \psi & 0 & 0 \end{bmatrix}, \quad (5)$$

$$\mathbf{A}_0^T = [0 \ 0 \ V], \quad (6)$$

The equations of motion of non-holonomic systems can be determined by means of several methods. For example, the extended version of the Lagrange equation of the second kind (also called as Routh-Voss equations in Gantmacher (1975)) is applicable but the elimination of the involved Lagrange-multipliers can lead to extensive algebraic manipulation. Here we rather apply the Gibbs-Appell method (see in Gantmacher (1975)), what is a more efficient approach since it provides the equations of motion in the form of first order differential equations. However, the definition of the pseudo velocities have to be chosen intuitively and the so-called energy of acceleration is also an unusual physical quantity.

We have three kinematic constraints and four generalized coordinates, which means that only one pseudo velocity has to be chosen:

$$\sigma := \dot{\varphi}, \quad (7)$$

which is the angular speed of the skater around the longitudinal axis of the skateboard. The generalized velocities can be expressed with the help of this pseudo velocity and the generalized coordinates:

$$\begin{bmatrix} \dot{X} \\ \dot{Y} \\ \dot{\psi} \\ \dot{\varphi} \end{bmatrix} = \begin{bmatrix} V \cos \psi \\ V \sin \psi \\ -\frac{V}{l} \tan \kappa \sin \varphi \\ \sigma \end{bmatrix}. \quad (8)$$

During the derivation of the equation of motion, the so-called energy of acceleration \mathcal{A} is needed. Since the model consists of one mass point only it can easily be computed:

$$\mathcal{A} = \frac{1}{2} m \mathbf{a}_C \cdot \mathbf{a}_C, \quad (9)$$

where \mathbf{a}_C refers to the acceleration of the lumped mass. In our model we obtain:

$$\mathcal{A} = \frac{1}{2} m h \frac{V^2}{l^2} \tan^2(\kappa) \sin^2(2\varphi) (l - h \tan(\kappa) \sin^2 \varphi) \dot{\sigma} + \frac{1}{2} m h^2 \dot{\sigma}^2 + \dots \quad (10)$$

According to the Gibbs-Appell method, the parts of the energy acceleration, which do not depend on the pseudo acceleration $\dot{\sigma}$, are not necessary to calculate and they are not computed here. The Gibbs-Appell equation forms as

$$\frac{\partial \mathcal{A}}{\partial \dot{\sigma}} = \Gamma, \quad (11)$$

where the right hand side is the pseudo force Γ . It can be determined from the virtual power of the active forces. In our model, the gravitational force and the control torque have non-zero virtual power, so they contribute to the pseudo force.

The equation of the motion of the system can be written as

$$\begin{aligned}\dot{\sigma}(t) &= \frac{g}{h} \sin(\varphi(t)) + \frac{DV}{mh^2} \sin(\psi(t-\tau)) + \frac{P}{mh} Y(t-\tau) - \\ &\quad - \frac{V^2}{lh} \tan(\kappa) \sin(\varphi(t)) \cos(\varphi(t)) \left(1 + \frac{h}{l} \tan(\kappa) \sin^2(\varphi(t))\right), \\ \dot{X}(t) &= V \cos(\psi(t)), \\ \dot{Y}(t) &= V \sin(\psi(t)), \\ \dot{\psi}(t) &= -\frac{V}{l} \tan(\kappa) \sin(\varphi(t)), \\ \dot{\varphi}(t) &= \sigma(t).\end{aligned}\tag{12}$$

The first equation of (12) relates to the Gibbs-Appell equation, the others are the formulas of the generalized velocities as the function of the pseudo velocity and the generalized coordinates. It is worth to mention that X is a so-called cyclic coordinate, so the second equation is unnecessary for further investigation. It means that the system can be described in the four dimensional state space.

3. STABILITY ANALYSIS OF THE RECTILINEAR MOTION IN CASE OF ZERO TIME DELAY

In this section, the linear stability analysis of the rectilinear motion is investigated in that special case, when the time delay of the control-loop is zero ($\tau = 0$). This theoretical case can be used for better understanding of the interaction of the skateboard and the skater. The linearized equation of motion around the stationary solution: $\sigma \equiv 0$, $Y \equiv 0$, $\psi \equiv 0$ and $\varphi \equiv 0$, can be written in the following form:

$$\begin{bmatrix} \dot{\sigma}(t) \\ \dot{Y}(t) \\ \dot{\psi}(t) \\ \dot{\varphi}(t) \end{bmatrix} = \begin{bmatrix} 0 & \frac{P}{mh} & \frac{DV}{mh^2} & \frac{g}{h} - \frac{V^2}{lh} \tan(\kappa) \\ 0 & 0 & \frac{V}{l} & 0 \\ 0 & 0 & 0 & -\frac{V}{l} \tan(\kappa) \\ 1 & 0 & 0 & 0 \end{bmatrix} \cdot \begin{bmatrix} \sigma(t) \\ Y(t) \\ \psi(t) \\ \varphi(t) \end{bmatrix}\tag{13}$$

The stability analysis of this linear ordinary differential equation system (13) can be carried out with the help of the Routh-Hurwitz criterion. The so-called Hurwitz matrix can be constructed from the coefficients of the characteristic equation. The i th sub-determinant of this Hurwitz matrix is denoted by Δ_i and the investigated equilibrium is asymptotically stable if and only if all of the sub-determinants Δ_i are greater than zero. Here $\Delta_0 = 0$, which means that the rectilinear motion can be stable only in Lyapunov sense but not exponentially stable. To achieve this stability, the following three conditions have to also be fulfilled:

$$\begin{aligned}-\frac{DV^2}{mh^2l} \tan(\kappa) &> 0, & -\frac{D^2V^4}{h^4l^2m^2} \tan^2(\kappa) &> 0, \\ \text{and } \frac{PV^2}{mh^2l} \tan(\kappa) &> 0.\end{aligned}\tag{14}$$

The second condition cannot be satisfied for any real parameters. This means that the rectilinear motion is unstable, or it can be stable in Lyapunov sense only if P and D are zeros. This result was examined by means of numerical simulations only. The analytical proof can be the subject of future work.

4. STABILITY ANALYSIS OF THE RECTILINEAR MOTION FOR NON-ZERO TIME DELAY

Let us investigate the more realistic case, when the skater's reflex delay is considered. From mathematical view point, this case is more complicated, because the system is governed by delay differential equations (DDEs). The linear stability analysis can be carried out based on the results of Stepan (1989).

The small vibrations of the board around the rectilinear motion can be described by the linearized equation:

$$\dot{\mathbf{X}}(t) = \mathbf{J} \cdot \mathbf{X}(t) + \mathbf{T} \cdot \mathbf{X}(t-\tau),\tag{15}$$

where

$$\mathbf{J} = \begin{bmatrix} 0 & 0 & 0 & \frac{g}{h} - \frac{V^2}{hl} \tan \kappa \\ 0 & 0 & V & 0 \\ 0 & 0 & 0 & -\frac{V}{l} \tan \kappa \\ 1 & 0 & 0 & 0 \end{bmatrix}, \quad \mathbf{X}(t) = \begin{bmatrix} \sigma(t) \\ Y(t) \\ \psi(t) \\ \varphi(t) \end{bmatrix},\tag{16}$$

$$\text{and } \mathbf{T} = \begin{bmatrix} 0 & \frac{P}{mh} & \frac{DV}{mh^2} & 0 \\ 0 & 0 & 0 & 0 \\ 0 & 0 & 0 & 0 \\ 0 & 0 & 0 & 0 \end{bmatrix}.$$

The characteristic function of this linear system can be calculated after the substitution of the exponential trial solution with characteristic exponent λ into (15):

$$\begin{aligned}D_c(\lambda) &= \lambda^4 + \lambda^2 \left(\frac{V^2}{hl} \tan \kappa - \frac{g}{h} \right) + \\ &\quad + e^{-\lambda\tau} (\lambda D + P) \frac{V^2}{mh^2l} \tan \kappa.\end{aligned}\tag{17}$$

The rectilinear motion is asymptotically stable if all of the infinitely many characteristic roots are situated on the left half of the complex plane. The limit of stability corresponds to the case when characteristic roots are located on the imaginary axis. If both the real and the imaginary parts of the characteristic exponent are zeros then saddle-node (SN) bifurcation can occur. In our case, $D_c(\lambda = 0) = 0$ leads to

$$\frac{P}{mh} \frac{V^2}{hl} \tan \kappa = 0\tag{18}$$

which gives a vertical line in the $P - D$ parameter plane:

$$P_{SN} = 0.\tag{19}$$

If only the real parts of the characteristic exponent are zero, Hopf bifurcation (H) can occur, and the characteristic exponent located on the imaginary axis can be expressed as $\lambda = \pm i\omega$, where i is the imaginary unit and $\omega \in \mathbb{R}^+$. The D-subdivision method can be used to determine the corresponding stability boundaries, namely, the characteristic equation has to be separated into real and imaginary parts:

$$\begin{aligned}0 &= \omega^4 + \omega^2 \left(\frac{g}{h} - \frac{V^2}{hl} \tan(\kappa) \right) + \\ &\quad + \left(\frac{D}{mh} \omega \sin(\omega\tau) + \frac{P}{mh} \cos(\omega\tau) \right) \frac{V^2}{hl} \tan(\kappa), \\ 0 &= \left(\frac{D}{mh} \omega \cos(\omega\tau) - \frac{P}{mh} \sin(\omega\tau) \right) \frac{V^2}{hl} \tan(\kappa).\end{aligned}\tag{20}$$

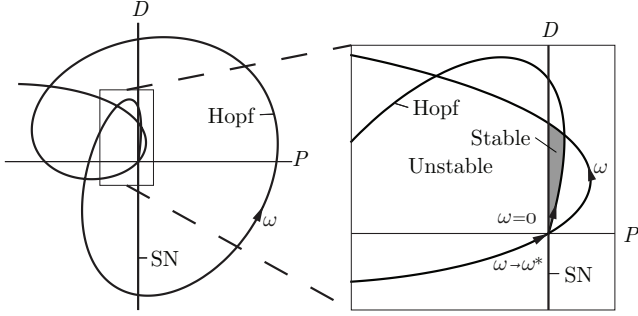


Fig. 3. Structure of stability chart for an arbitrary chosen longitudinal speed V and for the realistic parameters given in Table 1.

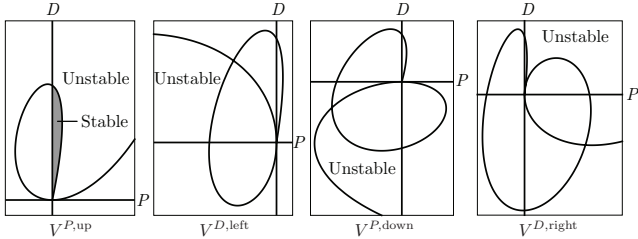


Fig. 4. Rotation of enclosed possible stable domain at certain speeds for the realistic parameters of Table 1.

The critical P and D parameters can be expressed as:

$$P_H = mh \frac{-hl}{V^2 \tan(\kappa)} \left(\omega^2 + \frac{g}{h} - \frac{V^2}{hl} \tan(\kappa) \right) \omega^2 \cos(\omega\tau),$$

$$D_H = mh \frac{-hl}{V^2 \tan(\kappa)} \left(\omega^2 + \frac{g}{h} - \frac{V^2}{hl} \tan(\kappa) \right) \omega \sin(\omega\tau). \quad (21)$$

Using the stability boundaries (19) and (21), a stability chart is constructed in the $P-D$ parameter plane in Figure 3. The vertical line of the SN bifurcation and the curve of the Hopf bifurcation terminate the linearly stable (shaded) and unstable (white) domains.

The stability boundary given by (21) starts from the origin, i.e. $P=0$ and $D=0$ for $\omega=0$. It can be proved that this curve can go through the origin for $\omega > 0$ if

$$V \geq V^* = \sqrt{\frac{gl}{\tan \kappa}}. \quad (22)$$

For realistic system parameters (see Table 2) $V^* = 1.403$ m/s. Let us not here, the rectilinear motion is unstable if $V < V^*$. The corresponding angular frequency can be determined as well:

$$\omega^* = \sqrt{\frac{V^2}{hl} \tan \kappa - \frac{g}{h}}. \quad (23)$$

If the speed is higher than the critical value V^* , the stability boundary curve intersects itself and a closed loop appears. It can be proved that only the inner part of this loop can be stable.

To describe the behavior of this closed loop is important, because this loop can cut of the stability region (see Figure 3.), for some parameters the stable region is vanished. One can verify that the above described closed loop of the stability boundary rotates counterclockwise around the origin of the $P-D$ parameter plane as the longitudinal

Table 1. Parameters of the skater-board system

h [m]	m [kg]	a [m]	τ [s]
0.85	75	0.05	0.24
s_t [Nm/rad]	l [m]	κ [°]	g [m/s ²]
100	0.3937	63	9.81

speed V increases. Since the angular frequency ω^* is also known, four specific speeds can be determined analytically, which relate to the special positions of the closed loop, i.e. when the loop is tangential with the axes of the $P-D$ plane. These positions are illustrated in Figure 4 and the corresponding critical speeds are:

$$V^{P,up} = \sqrt{(2k+1)^2 \frac{\pi^2}{\tau^2} + \frac{g}{h}} \sqrt{\frac{hl}{\tan \kappa}}, \quad (24)$$

$$V^{D,left} = \sqrt{\left(2k + \frac{3}{2}\right)^2 \frac{\pi^2}{\tau^2} + \frac{g}{h}} \sqrt{\frac{hl}{\tan \kappa}}, \quad (25)$$

$$V^{P,down} = \sqrt{(2k+2)^2 \frac{\pi^2}{\tau^2} + \frac{g}{h}} \sqrt{\frac{hl}{\tan \kappa}}, \quad (26)$$

$$V^{D,right} = \sqrt{\left(2k + \frac{1}{2}\right)^2 \frac{\pi^2}{\tau^2} + \frac{g}{h}} \sqrt{\frac{hl}{\tan \kappa}}, \quad (27)$$

where $k \in \mathbb{N}$.

According to the SN stability boundary at $P=0$, only the right hand side of $P-D$ parameter plane can be stable. If the stability boundary given in (21) starts to the left side of the $P-D$ plane at $\omega=0$ then no stable domain exists. It can also be proved that if this boundary starts to the right then stable domain can be located in the first quadrant.

Stable region exists if and only if the loop of the stability boundary has an intersection with its initial segment (often referred to D-curve, see for example, in Stepan (2009)). If this condition is satisfied then the Hopf boundary curve starts to the right side of the parameter plane, too. Accordingly, speed ranges can be determined, where stable domain exist:

$$\sqrt{\frac{r_k^2}{\tau^2} + \frac{g}{h}} < \frac{V_{s,k}}{\sqrt{\frac{hl}{\tan \kappa}}} < \sqrt{\left(2k + \frac{3}{2}\right)^2 \frac{\pi^2}{\tau^2} + \frac{g}{h}}. \quad (28)$$

Here, r_k is the k th root of equation $\tan r = r$ for $k \in \mathbb{N}$. The time delay also has to satisfy the condition:

$$\frac{r_k}{\sqrt{\frac{V^2}{hl} \tan \kappa - \frac{g}{h}}} < \tau_{s,k} < \frac{2\pi k + \frac{3}{2}\pi}{\sqrt{\frac{V^2}{hl} \tan \kappa - \frac{g}{h}}}. \quad (29)$$

The lower limit belongs to the geometric case on $P-D$ parameter plane, when the tangent of the Hopf boundary curve at ω and at ω^* are the same and the closed loop touches from below. The higher one belongs to the case when the closed loop just leaves the possibly stable domain (which is bounded by the D-shaped initial segment and the SN line), namely, the Hopf boundary curve touches the vertical axes from right at ω^* .

Thus, there are speed (or reflex delay) ranges, where the rectilinear motion is stable. Using the realistic parameters of Table 1 and assuming that the reflex delay of the skater is around 0.3 sec, the stable speed ranges can be calculated, see Table 2.

Table 2. Stabilizable speed domains

$1.40281 \text{ m/s} < V_{s,0} < 6.63623 \text{ m/s}$
$10.7254 \text{ m/s} < V_{s,1} < 15.1995 \text{ m/s}$
$19.4119 \text{ m/s} < V_{s,2} < 23.8243 \text{ m/s}$

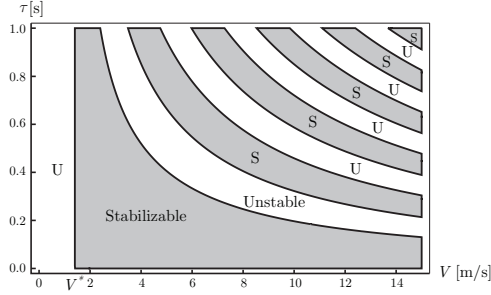


Fig. 5. Stabilizable domains in the space of the longitudinal speed V and reflex delay τ

As Table 2 and Figure 5 show, there are speed domains with low and higher values, where the control of the skateboard is not feasible. Naturally it does not mean, that the skater will fall, different control law can allow the skater to balance itself and keep the vertical position (see Varszegi et al. (2014), Kremnev and Kuleshov (2008) or Hubbard (1980)). However, the skater cannot follow the straight line by the skateboard. In Figure 5, the reflex delay τ can be seen against the longitudinal speed V . Shaded domains are stabilizable, which means that the rectilinear motion can be stable for appropriately chosen control gains P and D . This stability chart and the condition (28) do not contradict to the fact that the investigated equilibrium cannot be stable for $V < V^*$. Namely, the left inequality of (28) for $k = 0$ leads to the same condition. If $\tau = 0$, the system is at the edge of stability, the motion is unstable or it can be stable in Lyapunov sense but not exponentially stable.

If the control is switched off (the control gains are zeros) then the rectilinear motion is at the edge of stability if $V > V^*$. For $V < V^*$ the rectilinear motion is unstable (see in Hubbard (1980) or Kremnev and Kuleshov (2008)). This behavior can be observed in Figure 7, where the maximal allowable control gains P (dashed-dotted line) and D (dashed line) are plotted against the longitudinal speed. Figure 6 provides a better overview about the shapes of the stable domains in the space of the speed V and the control gains P and D . These last two figures were constructed with the parameters from Table 1. Without the variation of the control gains, small P and D parameter pairs seem to be the best choice from stability point of view, namely, they can guarantee the stability of the rectilinear motion in the largest speed domains.

5. CONCLUSION

A mechanical model of the skateboard-skater system was constructed, in which the effect of the human control was taken into account. The control law was demanded to move the board along an appointed straight line. The linear PD controller was considered with and without time delay. It was shown that the delay in the control loop is essential, namely, in case of non-zero time delay the rectilinear motion of the skateboard can be asymptotically

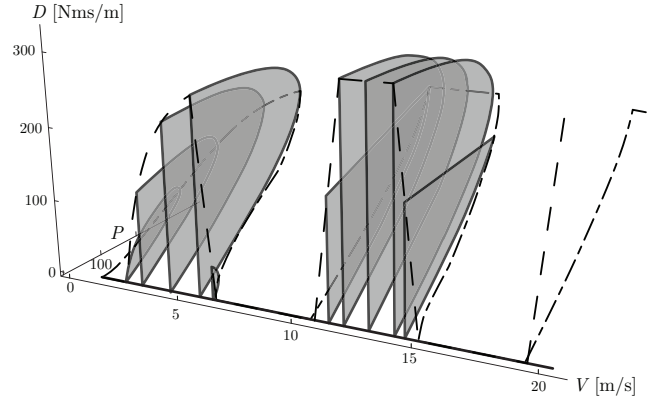


Fig. 6. Stability chart in the V - P - D parameter space

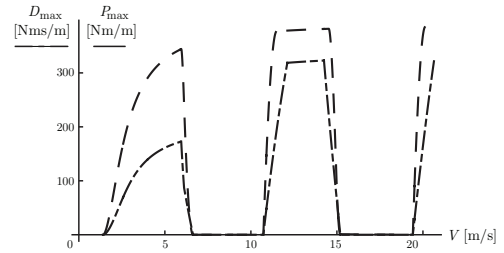


Fig. 7. The maximum allowable control gains against the speed

stable in some speed ranges. In case of zero time delay, the rectilinear motion can be stable in Lyapunov sense only, it is at the limit of stability.

The effect of the longitudinal speed was analyzed. The presented stability charts can explain the loss of stability even at low and high speeds. It was shown, that the skater must vary the control gains as the speed of the board changes. The stabilization of the board along an appointed straight line is possible in specific speed ranges. Out of these ranges, another control strategy is required, for example, instead of following of the appointed line, the balancing of the upper position is a successful strategy. Switching off the control is another solution, by which the motion can be kept at the limit of stability.

ACKNOWLEDGEMENTS

This research was partly supported by the János Bolyai Research Scholarship of the Hungarian Academy of Sciences and by the Hungarian National Science Foundation under grant no. OTKA PD105442.

REFERENCES

- Gantmacher, F. (1975). *Lectures in Analytical Mechanics*. MIR Publisher, Moscow, Russia.
- Hubbard, M. (1980). Human control of the skateboard. *Journal of Biomechanics*, 13, 745–754.
- Insperger, T. and Milton, J. (2014). Sensory uncertainty and stick balancing at the fingertip. *Biological Cybernetics*, 108, 85–101.
- Kremnev, A. and Kuleshov, A. (2008). Dynamics and simulation of the simplest model of skateboard. In *Proceedings of Sixth EUROMECH Nonlinear Dynamics Conference*. Saint Petersburg, Russia.

- Stepan, G. (1989). *Retarded dynamical systems: stability and characteristic functions*. Longman Scientific & Technical, London, United Kingdom.
- Stepan, G. (2009). Delay effects in the human sensory system during balancing. *Philosophical Transactions of The Royal Society*, 367, 1195–1212.
- Varszegi, B., Takacs, D., Stepan, G., and Hogan, S. (2014). Balancing of the skateboard with reflex delay. In *Proceedings of Eighth EUROMECH Nonlinear Dynamics Conference, ENOC2014*. Vienna, Austria.
- Wisse, M. and Schwab, A. (2005). Skateboard, bicycles, and three-dimensional biped walking machines: Velocity-dependent stability by means of lean-to-yaw coupling. *The International Journal of Robotics Research*, 24(6), 417–429.